

# Electron Probe Microanalyzer and Its Application To Ferrous Metallurgy

by R. Castaing, J. Philibert, and C. Crussard

**A**PPARATUS described in this paper uses the properties of X-radiation, emitted by substances under electron bombardment, as a means of rapid chemical point analysis. The method is based upon the principles of emission X-ray spectrography pioneered by Moseley in 1913.

A very finely focused beam of electrons—the *electron probe*—is projected on the surface of a sample, which has a very large area compared with the beam diameter, at the point where it is desired to know the chemical composition. The minute volume of the sample which is thus irradiated emits a complex X-ray spectrum consisting principally of the characteristic radiations of the elements present in the volume. Measurement of the wavelength and intensity of each component of this spectrum thus affords a simple method of determining the chemical identity and concentration of these elements.

The volume of sample which is analyzed at each position of the beam is limited by the diffusion of electrons in the sample. For an accelerating potential of the electron beam of about 30 kv, which is a convenient value for producing the characteristic radiation, this diffusion extends over a diameter of about  $1\ \mu$  normal to the beam, and about  $2\ \mu$  in the direction of the beam. Thus a beam of  $1\ \mu$  in diameter leads to a volume of about  $2\ \mu$  in diameter being irradiated. The limits of the analyzed region are thus considerably smaller than those obtained by using spark or arc emission spectrometry, which must extend to about  $50\ \mu$  at right angles to the beam, and those obtained in X-ray fluorescence analysis, where the penetration of the specimen is considerably greater.

The apparatus itself consists of three main parts: an electron optical system, an X-ray spectrograph and an optical microscope. The electron optical system consists of a tungsten cathode emitting the electrons, and a pair of magnetic lenses which focus the electron beam on the specimen to be analyzed. The specimen is prepared in the usual way, as in optical micrography. The X-radiation, emitted at the focal

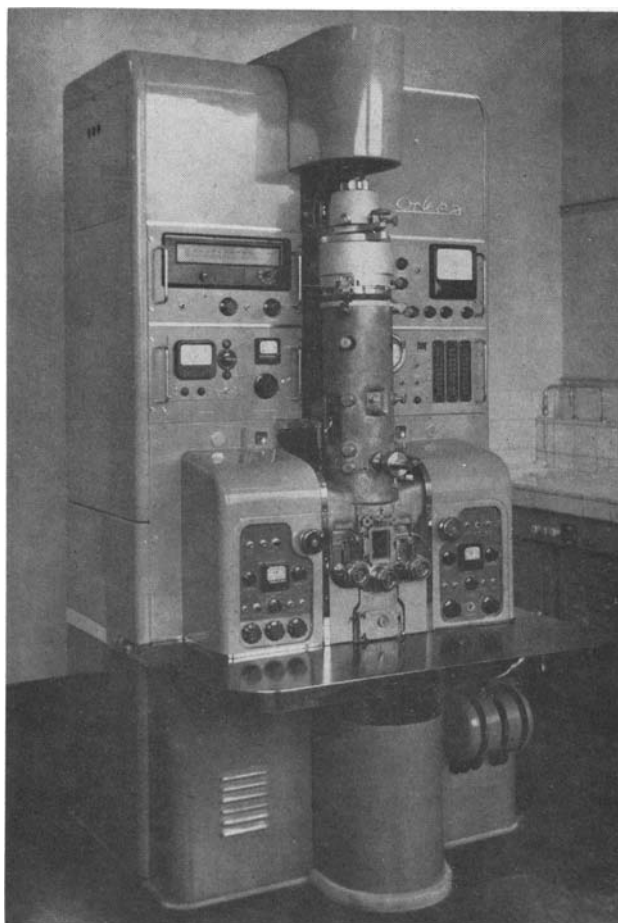


Fig. 1—General layout of the electron probe microanalyzer.

spot where the electrons strike the sample, is analyzed with a curved crystal, Geiger-Müller counter, vacuum spectrograph. The light microscope, designed to observe the surface of the sample in the region to be analyzed, is provided with a reflecting objective placed on the axis of the second magnetic lens. Its magnification is X450.

The quantitative determination of an element *A* in the analyzed region is made by measuring the intensity  $I_A$  of a strong characteristic line of the element, as emitted from the sample, and then the intensity  $I(A)$  of this same line as emitted from a

R. CASTAING is Professor, Faculté des Sciences, Université de Toulouse, Toulouse, France. C. CRUSSARD and J. PHILIBERT are Director of the Laboratories and Staff Member, respectively, Institut de Recherches de la Sidérurgie, Saint-Germain-en-Laye, France.

TP 4404E. Manuscript, June 26, 1956. New Orleans Meeting, February 1957.

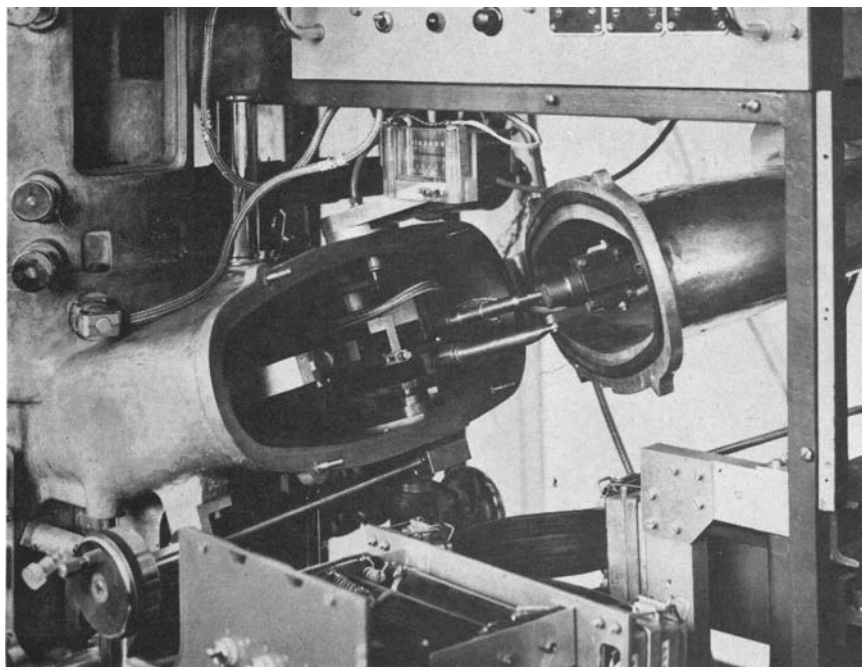


Fig. 2—View of the open spectrometer.

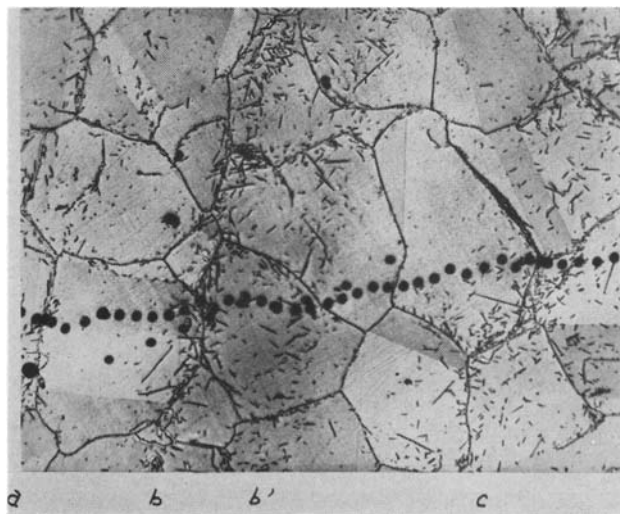


Fig. 3—Hadfield steel with segregation bands, annealed 2 hr at 850°C. Note that the impact spots are smaller than the black dots, due to a spreading of the contamination around the impact. Etched with nital. X450. Reduced approximately 35 pct for reproduction.

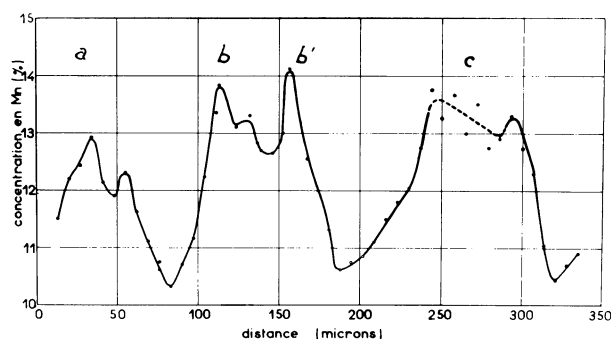


Fig. 4—Manganese segregation in Hadfield steel. Zones of high manganese content (a, b, b', and c) correspond to the carbide-containing bands, see Fig. 3.

piece of pure element  $A$  mounted near the sample. It can be shown, and this is one of the greatest advantages of this technique, that the ratio  $I_A/I(A)$  is to a first approximation equal to the concentration of element  $A$  in the sample. The comparison of these intensities of radiation of the same wavelength makes the method absolute, and avoids the use of standard alloys of composition covering a range of composition including that of the specimen. This factor is of prime importance if the method is to be of any practical use, since it would be impossible to make a series of standards which would be homogeneous on the small scale required for this technique.

An exact analysis requires that corrections for self-absorption in the specimen and fluorescence radiation be made. Graphs and equations giving these corrections have been established and, after due allowance, it is possible to obtain a precision of about 1 pct for chemical analyses.

The equipment described here, called hereafter a *microanalyzer*, enables the determination to be made of all the elements of atomic number greater than that of chlorine. It may be possible, by the use of special counters, to extend this limit downward in atomic number to include aluminium and magnesium. The analysis for very light elements, such as carbon, whose characteristic radiation is extremely soft, raises problems of technique which might make the method unsuitable for industrial use.

This method of rapid chemical analysis has already found many uses in the field of metallography, and may also be extended to the study of non-conductors, providing these are first coated with a very thin metallic layer (about  $3 \text{ m}\mu$  thick), which makes the surface conductive. Thus an important field of application is opened up in mineralogy. The study of certain elements in marine sediments has already been successfully carried out with this equipment.

It must be pointed out that the limit of resolution, normal to the beam, so far obtained (about  $2 \mu$ ), is not inherent in the method itself, but results from the use of relatively thick samples. If very thin samples were used, such as can be obtained by ionic bombardment through which the beam could pass

without scattering, this limit could be decreased still further without the technique becoming significantly more complicated.

### Construction of the Apparatus and Preliminary Trials

Two microanalyzers have been constructed at the Office National d'Etudes et Recherches Aéronautiques (ONERA) to the design of one of the authors.<sup>1,2</sup> The cost of construction was borne by ONERA and IRSID (Institut de Recherches de la Sidérurgie), each of which now has one complete model in operation. The layout of the apparatus is shown in Figs. 1 and 2.

The remainder of this paper is devoted to a description of some preliminary tests which have been made at IRSID to establish some possible applications in metallurgy. These were confined to studies of segregation, diffusion, identification and analysis of metallic phases and, finally, the microanalysis of minerals.

**Segregation of Manganese**—Although manganese is reputed not to show major segregation, it has long been known from microradiographic studies that minor segregation occurs.<sup>3</sup> A typical case of this is to be found in the banded structure of steels that contain a rather high percentage of manganese. Quantitative information on the degree of manganese segregation can be obtained with the equipment described. For the purposes of illustration two steels have been chosen.

**Tire Steel:** The tire steel analyzed as follows: C, 0.55 pct; Mn, 1.05 pct; S, 0.026 pct; Si, 0.3 pct; P, 0.020 pct.

The Comstock etch, which reveals the segregation of phosphorus, showed the typical structure of the bands of segregation. It is interesting here to note the presence of sulfides in the high phosphorus zones. Table I shows the results of the authors' analyses for manganese and iron at different locations.

These results show that, besides the regions of high manganese content resulting from the presence of sulfides, there is a considerable increase of manganese in the metallic matrix in the regions where phosphorus segregates.

**Hadfield Steel (12 Pct Mn, 1.28 Pct C):** A thorough investigation of the decomposition of austenite in this steel<sup>4-6</sup> has led to the conclusion that manganese segregation should be important in this steel. For

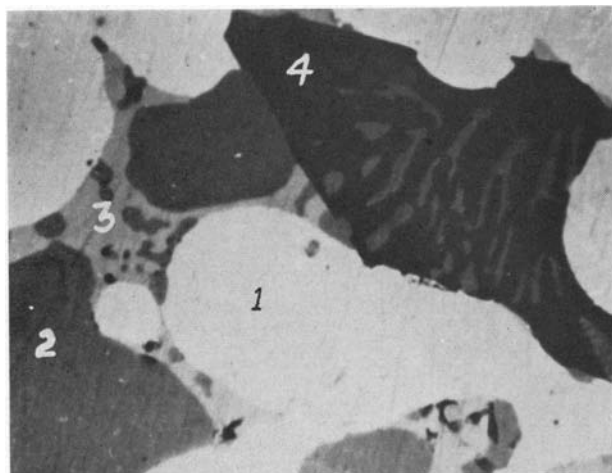


Fig. 5—Open-hearth steel scale; mechanical polishing. 1) metal; 2) FeO, ash grey; 3) FeS, yellowish grey; and 4) dark grey silicate. X1200. Reduced approximately 30 pct for reproduction.

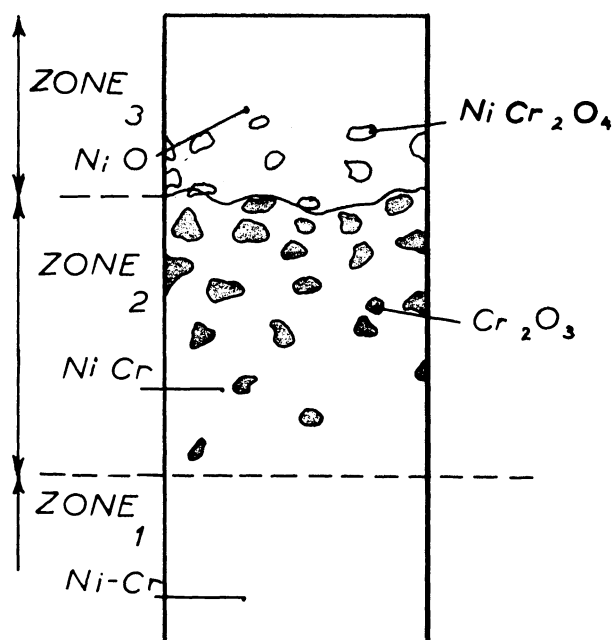


Fig. 6—Schematic diagram of oxidation of a Ni-Cr alloy.

that purpose, sections parallel to the axis of the rod have been examined by conventional micrography and with the microanalyzer. The banded structure is revealed markedly after an annealing at 850°C for 2 hr by carbides precipitated along some bands, as shown in Fig. 3.

A row of black dots seen in the same figure represents the successive impacts of the electron probe, when the sample has been analyzed in the apparatus. These impacts are due to contamination by an electron beam of increased intensity.

Segregation has been observed along that line, Fig. 4. Zones of high manganese content correspond

Table I. Manganese and Iron Contents

Analyzed Region	Pct Mn	Pct Fe
High phosphorus	1.4	
Medium phosphorus	0.9 to 1.1	
Low phosphorus	0.7	
Sulfide	42.5	20.5

to the carbide-containing bands, but it should be noted that the reported manganese content corresponds to that of the matrix, and not to that of the carbides, which are richer in manganese.

**Selective Oxidation During Scaling**—Scaling: Billets heated in an oil-fired furnace are coated with complex scales. With the microanalyzer, the various constituents can be studied, using a micrographic section. The photomicrograph of the interior of this scale, as found on a typical open-hearth billet (0.4 pct C, 0.6 pct Mn, 0.31 pct Si, 0.22 pct Ni, 0.14 pct Cu), shows the existence of four phases, Fig. 5. The results of the analyses, shown in Table II, enable the phases from the iron (+ manganese) content to be identified, the approximate composition of the phases being known in advance. The identifications are given in the last column of the table.

Considerable enrichment of nickel has been observed in the metal which is surrounded by oxides, sulfides, and silicates, whereas those phases themselves contain no trace of nickel. An increase in the copper content has been found in the sulfide, while

Table II. Results of Analyses

Analyzed Region	Pct Fe	Pct Mn	Pct Ni	Pct Cu	Total of Metals	Identification
1—White	96	0	3	0.75	100	Metal Oxide:FeO
2—Ash grey	77	≤0.5	0	0	77 to 77.5	
3—Yellowish grey	62	≤0.5	0	0.8	63 to 63.5	Sulfide:FeS Silicate
4—Dark grey	52	1 to 1.5	0	0	53	

none was observable in the oxide or in the silicate. Finally, manganese was found in the silicate.

**Internal Oxidation of Ni-Cr Alloys:** In the field of studies of the oxidation mechanism of binary alloys of iron, nickel, or chromium,<sup>6</sup> analyses have been made of the products of oxidation of a Ni-Cr alloy (4.6 pct Cr). A section, perpendicular to the surface, shows three distinct zones: 1) metal, 2) metal + precipitates of  $\text{Cr}_2\text{O}_3$ , and 3) dense oxide, Fig. 6.

From the analysis of zone 2 it has been verified that the only metal in the precipitates is chromium. In the metallic matrix the percentage of nickel varies progressively from 95 pct near zone 1 to 99 or 99.5 pct near the oxide zone 3, which corresponds to a decrease in chromium due to  $\text{Cr}_2\text{O}_3$  precipitation.

**Identifying and Studying the Phase-Equilibrium Diagrams**—It has been shown above, in the study of the scaling of billets, that the microanalyzer can be used for identifying phases of nearly stoichiometric compounds. Further examples of this will be given for various substances, e.g., sulfides and carbides. It should be noted here that the microanalysis of two phases in equilibrium makes the establishment of the equilibrium diagram possible with considerably fewer samples than with any previous method.

**Sulfides:** Microanalyses have been made of two types of sulfides encountered in cast iron. The yellowish grey sulfides, the so-called *iron-sulfides*, contain 60 to 61 pct Fe and 2 to 3 pct Mn. The ash grey sulfides, or *manganese-sulfides*, contain 43 to 25.5 pct Mn and 20 to 37.5 pct Fe. In both cases the total metal content is always about 63 pct. It is important to note that the iron-sulfide contains hardly any manganese, while the manganese-sulfide

often has a higher percentage of iron than of manganese.

**Carbides:** In high-alloy steels the microanalyzer can be used to follow the growth of carbides during high-temperature heat treatment.

A. High Speed Steel. Analyses have been made of samples used (by J. Papier) in a study of high-speed steel of the type 18-4-2.<sup>7</sup> The analysis of this steel gave, in weight percent: C, 0.8; W, 18.8; Cr, 4.4; and V, 1.9.

Here again a direct study of the metallic matrix was made whereas, in the usual method, which uses electrolytic extraction of carbides, the composition of the matrix has to be determined by difference.

The samples have been treated in two ways: annealing at 1300° and at 1050°C. In the first case, the carbides were relatively large (about 5  $\mu$ ), while in the second case their dimensions were as small as the limit of resolution of the microanalyzer. Three elements, iron, tungsten, and chromium, have

Table III. Results of Analyses

Temperature of Heat Treatment	Phase	Pct Fe	Pct W	Pct Cr	Total
1300°C	{ Matrix	84.5	8.5	5	98
	{ Carbide	31.5	60	3	94.5
1050°C	{ Matrix	87.5	5.5	5	98
	{ Carbide	31.5	56	3	90.5

been determined, and analyses for vanadium will be carried out shortly.

The results in Table III refer to the complex carbides of tungsten and to the matrix, excluding the small carbides (of vanadium).

B. Austenitic Steel for Turbine Blades. Small precipitates were observed on a micrographic specimen of an austenitic steel (for turbine blades) containing nickel, chromium, and cobalt, and a small percentage of molybdenum, tungsten, and columbium; these were carbides of columbium, this element being found in the precipitates only and not in the matrix. It was immediately verified that this was columbium and not tantalum.

**Fe-Cr Alloys:** The results of G. Pomey on the  $\sigma$ -transformation of Fe-Cr alloys<sup>8,9</sup> show that for a 45 pct pure chromium alloy the percentage of iron and chromium in the  $\alpha$  and  $\sigma$ -phases ( $\sigma$  formed by cold-working) are equal. These results have been confirmed. Thus, the transformation takes place without diffusion.

By maintaining the temperature at 1050°C and using impure alloys, complex carbides of iron and of chromium can be formed, which redissolve only above 1200°C. For a 30 pct Cr alloy, annealed at 1050°C, Fig. 7, it was found that the matrix was only slightly impoverished (28.5 pct Cr) but, within 4 to 5  $\mu$  of the carbides, the percentage of chromium

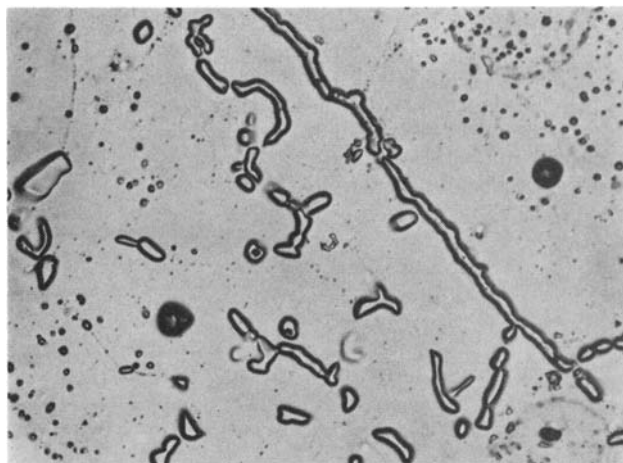


Fig. 7—Fe-30 pct Cr alloy annealed at 1050°C. Ferrite and carbides; electrolytic polishing. X700. Reduced approximately 30 pct for reproduction.

went down to 26 pct. The analysis gave the following composition for the carbide: 59 pct Cr and 31 pct Fe, which probably corresponds to the carbide  $M_7C_3$ .

**Studies of Diffusion**—The microanalyzer is especially useful in studying the interdiffusion between two metals, or alloys, at high temperature. With this apparatus, the penetration curves can be traced rapidly and with a high degree of accuracy. Two studies are now being pursued: one concerning the diffusion couple Fe-Cu; the other, in collaboration with the Atomic Energy Commission, concerning the couple U-Zr. From these curves the diffusion coefficients, their variation with concentration, the activation energy, and (for diffusion in multiple phases) the limits of solubility, can be obtained.

Both concentration penetration curves are given here in order to indicate the high degree of precision the method can yield.

1) For a general study of U-Zr diffusion, U-Zr couples formed by welding at 600°C under a high pressure have been utilized, and diffusion curves obtained in the temperature range where  $\gamma$ -uranium dissolves in all proportions in  $\beta$ -zirconium.<sup>10</sup>

Fig. 8 shows the penetration curve studied after a diffusion treatment of 4 hr at 1000°C. For these measurements, the  $K\alpha_1$  rays of zirconium and  $L\alpha_1$  rays of uranium were chosen. The diffusion coefficient was observed to vary considerably with the atomic concentration  $C$  of zirconium. The values of the diffusion coefficient at  $C = 10$  pct and  $C = 95$  pct are  $3.2 \times 10^{-10}$  sq cm per sec and  $8.0 \times 10^{-10}$  sq cm per sec, respectively; the diffusion coefficient is also seen to pass through a minimum of  $4.3 \times 10^{-10}$  sq cm per sec at  $c = 80$  pct, Fig. 9.

2) The Fe-Cu couples were made by vacuum melting pure copper in pure iron crucibles above the temperature at which  $\epsilon$ -phase is formed, i.e., above 1094°C.<sup>11</sup>

The diffusion of copper in iron was seen to proceed mainly along grain boundaries. After quenching and etching, each grain is seen to be surrounded by a succession of differently colored rings. The copper concentration in these aureoles have been measured from the interface Fe-Cu or from grain boundaries to the interior of the grains. Fig. 10 shows the results obtained by a diffusion treatment of 64 hr at 1100°C. The solubility limit of copper in iron, measured very near the  $\gamma/\gamma + \text{liquid}$  interface, is seen to be 10 pct (in weight).

The penetration of copper in iron indicated in the graph is measured along a direction in the plane of

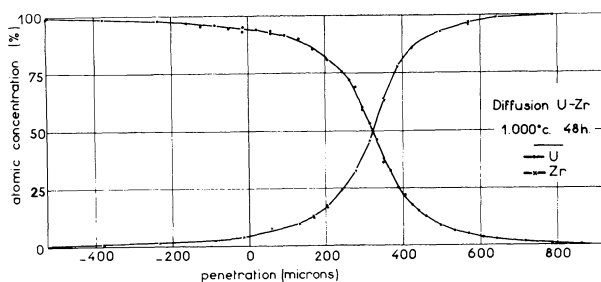


Fig. 8—Concentration-penetration curve of U-Zr diffusion for 48 hr at 1000°C.

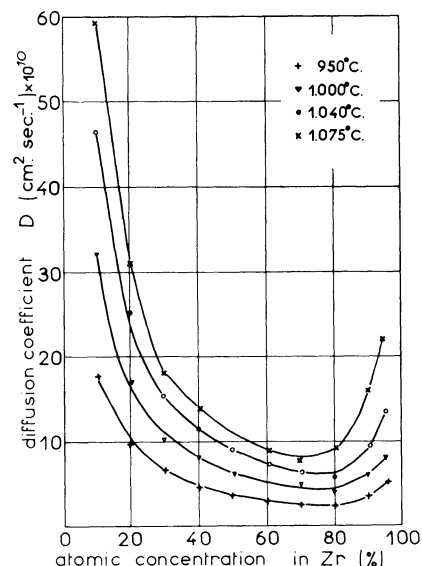


Fig. 9—Variation of the diffusion coefficient with atomic concentration in zirconium.

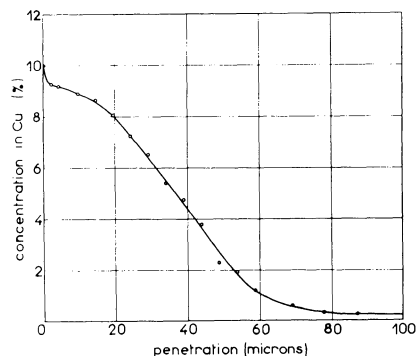


Fig. 10—Concentration-penetration curve of Cu-Fe; diffusion for 64 hr at 1100°C.

Table IV. Results of Oolite Analysis

Iron Ore	Analyzed Region	Fe, Pct
First oolite	Central nucleus	50.5
	Black zones	43.5 to 44.5
	White zones	48.5 to 49.5
	Grey zones	45.5 to 46.5
	Central nucleus	52.5
Second oolite	Black zones	42.5
	Dark grey zones	45.5 to 46.5
	White zones	48 to 49

observation, but this plane is oblique to the plane of the interface.

**Studies of Iron Ore**—It is possible to study non-conductors as well as metals, provided they receive a special preparation such as metallizing.

Oolites, extracted from a Lorraine ore, were studied in this manner. These were first embedded in

plastic, and mechanically polished, Fig. 11. Analyses of the iron contents were made of the nucleus and the various concentric layers of the oolite, Table IV. The percentage of manganese in oolite is too low to permit precise measurements; however, it seems that the zones which are richest in iron are also the richest in manganese.

## Conclusion

This short survey of the first results obtained with the fine-focus emission spectrometer demonstrates the great variety of its applications. It is possible to carry out local analyses of non-conductors (such as ores) as well as metals or alloys of one or more phases and, further, to measure all the variations of composition within one phase such as a segregate. The very light elements cannot be determined, as has been stated in the introduction. The microanalyzer has also been used to find the

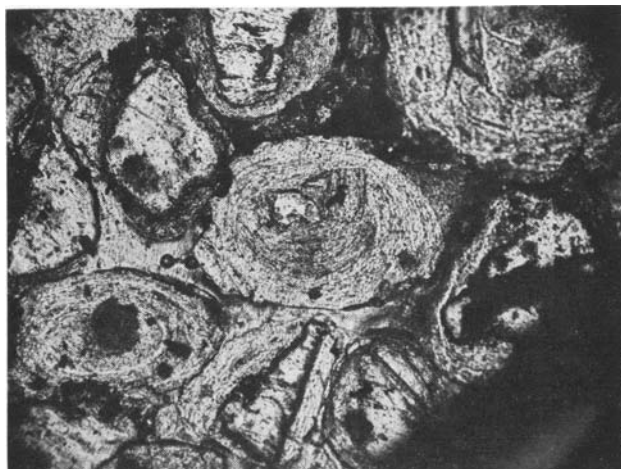


Fig. 11—Oolite from the ore of Sainte-Barbe, embedded in plastic and mechanically polished. X150. Reduced approximately 25 pct for reproduction.

composition of non-metallic inclusions, of sulfides, carbides, and oxides formed by internal or surface oxidation. By analyzing the surrounding matrix, the distribution coefficient of various elements be-

tween precipitates and matrix is automatically obtained. If the precipitates have been obtained by prolonged annealing at a fixed temperature, it is easy to establish the equilibrium diagram.

Experience has shown that the accuracy of these analyses is excellent. The relative error is about 1 pct for percentages which are not too low. The detection threshold of an element seems to be at concentrations of about 0.2 to 0.3 pct.

#### References

- <sup>1</sup> R. Castaing: Thesis, 1951. ONERA Publication No. 55.
- <sup>2</sup> R. Castaing and J. Descamps: *Le Journal de Physique et le Radium*, 1955, vol. 16, p. 304.
- <sup>3</sup> W. Betteridge and R. S. Sharpe: *Journal Iron and Steel Inst.*, London, 1948, vol. 158, p. 185.
- <sup>4</sup> A. Kohn, J. Plateau, and G. Pomey: *Comptes Rendus*, 1956, vol. 242, p. 256.
- <sup>5</sup> G. Collette, C. Crussard, A. Kohn, J. Plateau, G. Pomey, and M. Weisz: Communication to *Journée d'automne de la Sté Française de Métallurgie*, 1956.
- <sup>6</sup> J. Moreau and J. Benard: *Comptes Rendus*, 1953, vol. 237, p. 1417.
- <sup>7</sup> J. Papier: *Revue de Métallurgie*, 1954, vol. 51, p. 723.
- <sup>8</sup> G. Pomey and P. Bastien: *Revue de Métallurgie*, 1956, vol. 53, p. 147.
- <sup>9</sup> G. Pomey: Thesis, 1955. IRSID Publication No. A117.
- <sup>10</sup> Y. Adda and J. Philibert: *Comptes Rendus*, 1956, vol. 242, p. 3081; vol. 243, p. 1115.
- <sup>11</sup> M. Zumer and F. Sirca: *Rudarsko Metalurški Zbornik*, 1951, No. 1, p. 25.

Discussion of this paper sent (2 copies) to AIME by June 1, 1957 will appear in AIME Transactions Vol. 209, 1957, and in JOURNAL OF METALS, October 1957.

## Oxidation of Zirconium Between 400° and 800°C

The vacuum microbalance method is used to study the oxidation reaction for two surface preparations over the temperature range of 400° to 800°C. The results fit in well with the authors previous work at temperatures of 200° to 425°C and with the work of other groups at higher temperatures. An analysis of the rate data shows that the cubic rate law fits the experimental data best for the abraded specimens. However, the parabolic rate law can be fitted to the data if an initial deviation is disregarded. With chemically polished specimens, a good fit is obtained with the parabolic rate law. The parabolic rate law constant  $A$  gives two straight lines when plotted as  $\log A$  vs  $1/T$ . For the temperature range of 200° to 525°C an energy of activation of 18,200 cal per mol is calculated while a value of 28,600 cal per mol is calculated for the temperature range of 525° to 750°C. The results of this work bring together the previously determined high-temperature oxidation studies of Cubicciotti with the early low-temperature studies of Gulbransen and Andrew.

by Earl A. Gulbransen and Kenneth F. Andrew

DRY oxidation of zirconium has been studied by several groups.<sup>1-3</sup> The present work extends our early study<sup>1</sup> to the high-temperature studies of Cubicciotti<sup>2</sup> and Belle and Mallett.<sup>3</sup> Gulbransen and

Andrew<sup>1</sup> showed that the parabolic rate law fitted the 2-hr experiments between 200° and 425°C after an initial deviation. An energy of activation of 18,200 cal per mol was calculated. Cubicciotti,<sup>2</sup> in a study between 593° and 880°C, showed that the parabolic rate law fitted the data and an energy of activation of 32,000 cal per mol was calculated. In contrast to these studies on sheet specimens, Belle and Mallett<sup>3</sup> studied the oxidation reaction on rod specimens and found a cubic rate law to fit the data.

E. A. GULBRANSEN, Member AIME, and K. F. ANDREW are associated with the Research Laboratories, Westinghouse Electric Corp., Pittsburgh.

TP 4376E. Manuscript, July 9, 1956. New Orleans Meeting, February 1957.